7. A. A. Khalatov, "Integral method of calculating the development of a swirled stream in a channel," Izv. Vyssh. Uchebn. Zaved., Aviats. Tekh., No. 3 (1977).
8. A. A. Khalatov, V. K. Shchukin, V. G. Letyagin, and A. V. Kozhevnikov, "Friction law and form parameters of swirled flow in a cylindrical channel," Izv. Vyssh. Uchebn. Zaved., Aviats. Tekh., No. 3 (1977).
9. V. P. Ustimenko, Turbulent Transfer Processes in Rotating Flows [in Russian], Nauka, Alma-Ata (1977).
10. S. S. Kutateladze, B. P. Mironov, V. E. Nakoryakov, and E. M. Khabakhpasheva, The Experimental Investigation of Turbulent Boundary Flows [in Russian], Nauka, Novosibirsk (1975).
11. V. G. Letyagin, V. K. Shchukin, A. A. Khalatov, and A. V. Kozhevnikov, "Turbulence intensity in the flow of swirled streams in pipes," Dep. VIMI, Reg. No. VMD 02674 (annotated in Riport, No. 21, 1976).

MATHEMATICAL ANALYSIS OF WHIRLED TURBULENT FLOW THROUGH A PIPE

V. V. Tret'yakov and V. I. Yagodkin UDC 532.542.4

The effect of rotation of the stream on the development of turbulent flow in a pipe is analyzed by a numerical method. Calculated distributions of average turbulence velocity and energy are compared with experimental data.

Study of whirled turbulent flow is very important. Owing to the tremendous complexity of such a flow, however, it has so far been studied less extensively than similar flow without whirling. This applies especially to flow through pipes. Here will be presented the results of numerical calculations pertaining to whirled turbulent flow through a cylindrical pipe, calculations based on the two-parametric $k-\varepsilon$ and $k-W$ models of turbulence [1]. Various authors have used these models earlier for calculating the flow in boundary layers, in free or bounded jets, and through channels of intricate shapes. They compared the theoretical and experimental data on the basis of average flow characteristics (velocity profiles, size and location of the recirculation zone, etc.). In [2], e.g., a comparison is shown between calculated and measured profiles of average velocity along an annular channel. This is partly attributable to the fact that published experimental data on whirled flow are incomplete in terms of turbulence characteristics. For this reason, we have selected for comparison the data in [3] containing not only the profiles of the components of average velocity and the pressure distributions along the pipe wall as well as along the pipe axis, but also data on the distribution of and the correlation between the intensities of the three components of velocity fluctuations in the stream.

The system of equations describing a steady turbulent motion of an incompressible fluid through a pipe, under the assumption of a rotationally symmetric flow without external body forces acting and with constant molecular transfer coefficients, can be written in cylindrical coordinates as

$$\frac{\partial v_z}{\partial z}+\frac{1}{r}\frac{\partial}{\partial r}(rv_r)=0,$$

$$\frac{\partial v_z v_r}{\partial z}+\frac{1}{r}\frac{\partial r v_r^2}{\partial r}=\frac{\partial}{\partial z}\left[(\nu+\nu_t)\frac{\partial v_r}{\partial z}\right]+\frac{2}{r}\frac{\partial}{\partial r}\left[r(\nu+\nu_t)\frac{\partial v_r}{\partial r}\right]+\frac{\partial}{\partial z}\left[(\nu+\nu_t)\frac{\partial v_z}{\partial r}\right]-2(\nu+\nu_t)\frac{v_r}{r^2}+\frac{v_\theta^2}{r}-\frac{1}{\rho}\frac{\partial p}{\partial r},$$

$$\frac{\partial v_z^2}{\partial z}+\frac{1}{r}\frac{\partial r v_r v_z}{\partial r}=2\frac{\partial}{\partial z}\left[(\nu+\nu_t)\frac{\partial v_z}{\partial z}\right]+\frac{1}{r}\frac{\partial}{\partial r}\left[r(\nu+\nu_t)\frac{\partial v_r}{\partial z}\right]-\frac{1}{\rho}\frac{\partial p}{\partial z}+\frac{1}{r}\frac{\partial}{\partial r}\left[r(\nu+\nu_t)\frac{\partial v_z}{\partial r}\right], \quad (1)$$

$$\frac{\partial r v_z v_\theta}{\partial z}+\frac{1}{r}\frac{\partial r^2 v_r v_\theta}{\partial r}=\frac{\partial}{\partial z}\left[(\nu+\nu_t)\frac{\partial r v_\theta}{\partial z}\right]+\frac{1}{r}\frac{\partial}{\partial r}\left[r(\nu+\nu_t)\frac{\partial r v_\theta}{\partial r}\right]-\frac{2}{r}\frac{\partial}{\partial r}[(\nu+\nu_t)rv_\theta],$$

where v_z, v_r, and v_θ are time-averaged components of velocity.

Translated from Inzhenerno-Fizicheskii Zhurnal, Vol. 37, No. 2, pp. 254-259, August, 1979. Original article submitted September 5, 1978.

 0022-0841/79/3702-0920$07.50

For calculating the coefficient of turbulent viscosity ν_t we will use the transfer equations pertaining to the kinetic energy of turbulence per unit volume $k = \langle v_i'^2 \rangle /2$ and to the rate of its dissipation $\varepsilon = \nu \langle (\partial v_i'/\partial x_j)^2 \rangle$ in the $k-\varepsilon$ model as well as the transfer equations pertaining to quantities k and W in the $k-W$ model, quantity W being proportional to the frequency of turbulent fluctuations squared.

It has been demonstrated in [2] that, despite the experimentally observable anisotropy of the coefficient of turbulent viscosity [4], this coefficient can be regarded as a scalar quantity in calculations pertaining to the distribution of the average velocity of whirled flow through an annular channel. Accordingly, the coefficient ν_t will be calculated with the aid of the Kolmogorov – Prandtl relations

$$\nu_t = C_\mu k^2/\varepsilon, \tag{2}$$

$$\nu_t = kW^{-\frac{1}{2}} \tag{3}$$

in the turbulence models $k-\varepsilon$ and $k-W$, respectively, as well as the transfer equations for k, ε, and W in the

$$\begin{aligned}
\frac{\partial v_z k}{\partial z} + \frac{1}{r}\frac{\partial r v_r k}{\partial r} &= \frac{\partial}{\partial z}\left(\frac{\nu+\nu_t}{\sigma_k}\frac{\partial k}{\partial z}\right) + \frac{1}{r}\frac{\partial}{\partial r}\left(r\frac{\nu+\nu_t}{\sigma_k}\frac{\partial k}{\partial r}\right) + S_k,\\
\frac{\partial v_z \varepsilon}{\partial z} + \frac{1}{r}\frac{\partial r v_r \varepsilon}{\partial r} &= \frac{\partial}{\partial z}\left(\frac{\nu+\nu_t}{\sigma_\varepsilon}\frac{\partial \varepsilon}{\partial z}\right) + \frac{1}{r}\frac{\partial}{\partial r}\left(r\frac{\nu+\nu_t}{\sigma_\varepsilon}\frac{\partial \varepsilon}{\partial r}\right) + S_\varepsilon,\\
\frac{\partial v_z W}{\partial z} + \frac{1}{r}\frac{\partial r v_r W}{\partial r} &= \frac{\partial}{\partial z}\left(\frac{\nu+\nu_t}{\sigma_w}\frac{\partial W}{\partial z}\right) + \frac{1}{r}\frac{\partial}{\partial r}\left(r\frac{\nu+\nu_t}{\sigma_w}\frac{\partial W}{\partial r}\right) + S_w
\end{aligned} \tag{4}$$

form. The first terms on the right-hand side appear in the gradiental-diffusion approximation and the expressions for the source terms S_k, S_ε, and S_W are

$$\begin{aligned}
S_k &= \nu_t F_k - \varepsilon,\\
S_\varepsilon &= \varepsilon(C_{1,\varepsilon}\nu_t F_k - C_{2,\varepsilon}\varepsilon)/k,\\
S_k &= \nu_t F_k - C_\mu k\sqrt{W},\\
S_w &= C_{1,w}\nu_t(\mathrm{grad}\,\omega_i)^2 - C_{2,w}W^{3/2} + C_{3,w}\frac{W}{k}\nu_t F_k,\\
F_k &= 2\left[\left(\frac{\partial v_z}{\partial z}\right)^2 + \left(\frac{\partial v_r}{\partial r}\right)^2 + \frac{v_r^2}{r^2}\right] + \left(\frac{\partial v_\theta}{\partial z}\right)^2 + \left(r\frac{\partial}{\partial r}\frac{v_\theta}{r}\right)^2 + \left(\frac{\partial v_z}{\partial r} + \frac{\partial v_r}{\partial z}\right)^2,
\end{aligned} \tag{5}$$

with ω_i denoting the components of the velocity vortex. The values of the empirical constants in these equations are, according to data in [1, 5], $C_\mu = 0.09$ and $\sigma_k = 1.0$, $\sigma_\varepsilon = 1.3$, $C_{1,\varepsilon} = 1.44$, $C_{2,\varepsilon} = 1.92$ in the $k-\varepsilon$ model, and $\sigma_k = \sigma_W = 0.9$, $C_{1,w} = 3.5$, $C_{2,w} = 0.17$, $C_{3,w} = 1.04$ in the $k-W$ model.

The system of equations (1)-(5) will be solved by the finite-differences method [6], for which these equations are transformed by introduction of the flow function ψ and the tangential vortex component $\omega = \Omega r$

$$v_z = \frac{1}{\rho r}\frac{\partial \psi}{\partial r}, \quad v_r = -\frac{1}{\rho r}\frac{\partial \psi}{\partial z}, \quad \Omega = \frac{1}{r}\left(\frac{\partial v_r}{\partial z} - \frac{\partial v_z}{\partial r}\right) \tag{6}$$

in lieu of the pressure p and the velocity components v_z, v_r.

Inasmuch as equations describing such a flow are of the elliptic kind, the values of variables ψ, Ω, v_θ, k, and ε or W (depending on the model) must be determined at all boundaries of the flow region.

The profiles of each variable at the channel entrance section are stipulated arbitrarily and regarded as parameters of the problem. The profile of tangential velocity v_θ will, moreover, be stipulated according to the law for a solid body, this law approximating the profile experimentally established in [3].

The conditions at the axis of symmetry are stipulated as

$$\psi(r=0) = 0, \tag{7}$$

$$v_\theta(r=0) = 0, \tag{8}$$

$$\frac{\partial k}{\partial r} = \frac{\partial \varepsilon}{\partial r} = \frac{\partial W}{\partial r} = 0 \quad \text{at} \quad r = 0, \tag{9}$$

$$\Omega_P = -8\left[(\psi_{NNP} - \psi_P)/r_{NNP}^2 - (\psi_{NP} - \psi_P)/r_{NP}^2\right]/(r_{NNP}^2 - r_{NP}^2), \tag{10}$$

where expressions (7)-(9) represent conventional conditions of symmetry and where the boundary condition for Ω has been expressed in finite-difference form on the assumption that in the vicinity of the axis it is possible to expand functions ψ and Ω into Taylor series with respect to the distance from the axis as the parameter. Subscripts P, NP, and NNP refer to values of this function, respectively, on the axis and in the first and second radial layers of the finite-difference grid.

The constraints on all functions at the channel exit are stipulated as

$$\partial/\partial z = 0 \quad \text{at} \quad z = L. \tag{11}$$

Numerical calculations have shown that assuming the approximate boundary condition (11) affects the solution only in the immediate vicinity of the exit section. The numerical results which will be shown here refer to the region beyond this zone.

The constraint on the flow function at the solid boundary follows from the condition of zero leakage

$$\psi(r = r_0) = \text{const}, \tag{12}$$

with the value of the constant determined from the condition of normalizing with respect to the mean-discharge velocity v_m. The constraints on all other variables at the solid boundary are determined from the assumption that the "wall law" applies to a curved surface, this assumption having been validated by experimental data [7].

Accordingly, within layer Δ nearest to the solid surface one can assume

$$v_{\theta,\Delta} = \frac{1}{\varkappa} V_\theta^* \operatorname{Ln}\left(\frac{E\Delta V_\theta^*}{\nu \cos\alpha}\right), \tag{13}$$

$$\Omega_\Delta = \frac{V_* \sin\alpha}{r_\Delta \Delta\varkappa}, \tag{14}$$

$$k_\Delta = V_*^2 C_\mu^{-1/2}, \tag{15}$$

$$\varepsilon_\Delta = V_*^3 (\Delta\varkappa)^{-1}, \tag{16}$$

$$W_\Delta = C_\mu^{-1} (V_* \Delta^{-1} \varkappa^{-1})^2, \tag{17}$$

where

$$V_* = V_\theta^*/\cos\alpha = V_z^*/\sin\alpha, \quad \operatorname{tg}\alpha = v_z/v_\theta.$$

The values of V_z^* and V_θ^* are found from calculated values of the flow function ψ and the tangential velocity component v_θ, as solutions of the two transcendental equations

$$\frac{\partial\psi}{\partial r} = \frac{\rho r V_z^*}{\varkappa} \operatorname{Ln}\left(\frac{E V_z^* \Delta}{\nu \sin\alpha}\right), \quad v_\theta = \frac{V_\theta^*}{\varkappa} \operatorname{Ln}\left(\frac{E\Delta V_\theta^*}{\nu \cos\alpha}\right),$$

where $\varkappa = 0.41$ and $E = 9.0$.

Experimental data on the distributions of the three components of average velocity in a pipe are presented in [3] for two values of the whirl parameter $\sigma = \omega_0 r_0/v_m$: $\sigma = 0$ and $\sigma = 3$ (ω_0 denoting the average angular velocity of a gas at the exit from the whirler). The distributions of intensities of velocity fluctuations are shown for the same values of the whirl parameter. The experiments were performed with the Reynolds

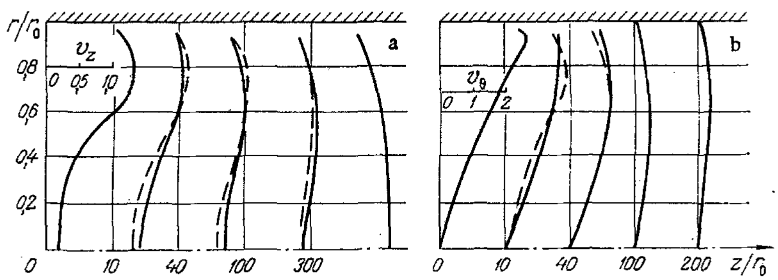

Fig. 1. Change of profiles along a pipe: a) profile of the axial velocity component v_z; b) profile of the tangential velocity component v_θ. N_{Re} $1.5 \cdot 10^4$. Solid lines represent calculations; dashed lines represent experimental data in [3].

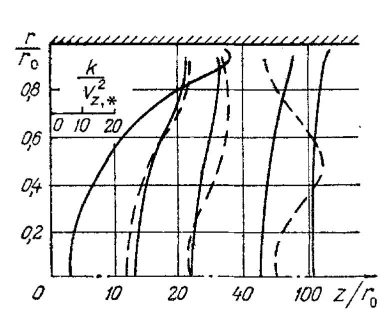

Fig. 2

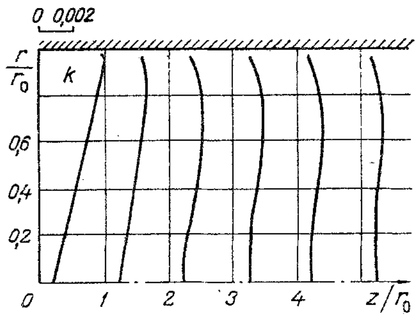

Fig. 3

Fig. 2. Change of the profile of turbulence energy k along a pipe. $N_{Re} = 1.5 \cdot 10^4$. Solid lines represent calculations; dashed lines represent experimental data in [3].

Fig. 3. Change of the profile of turbulence energy k along the initial pipe segment. $N_{Re} = 10^5$.

number $N_{Re} = v_m r_0/\nu$ equal to $1.5 \cdot 10^4$ and the dynamic velocity $V_* = 0.0545 v_m$. These data were compared with calculations for the same values of these parameters.

Calculations were made first for an unwhirled flow ($\sigma = 0$), assuming for the components of average turbulence velocity and energy at the pipe entrance conditions close to those experimentally established in [3]. Assumed was, furthermore, a uniform profile of turbulent viscosity ν_t.

The calculations revealed a profile of the axial velocity component developing into one close to the experimentally established one, but some discrepancies in the profiles of turbulence energy k. These discrepancies could arise due to the actual flow in this case not being fully developed within the initial segment of the pipe. With the turbulent flow fully developed further downstream ($z/r_0 \geq 150$), the profiles of v_z and k were found to approach those experimentally established in [8].

The next step was calculating a whirled flow ($\sigma = 3$), with the rotation of the stream significantly affecting the average values of the flow parameters and the turbulence characteristics. Calculations and experimental data pertaining to v_z, v_θ, and k within the entrance segment in this case are compared in Figs. 1 and 2. The calculations here are based on the k – W model. The graphs indicate a close agreement between calculated and measured distributions of both velocity components over the entire pipe length, but somewhat more discrepancy between the respective distributions of turbulence energy, especially within the $z/r_0 = 25$-60 zone. This discrepancy could be due to a loss of stability in a rotational flow by a mechanism generating additional turbulence energy in the stream but disregarded in both models. The results of calculations according to the k – ε model agree almost exactly with those based on the k – W model. Therefore, they correctly depict the flow pattern within the initial segment $L \leq (10\text{-}15)r_0$ and both models of turbulence are useful for describing a whirled turbulent flow such as the one considered here.

For the purpose of determining the effect of whirling on the distributions of kinetic turbulence energy and of components of the average velocity within the initial pipe segment, calculations were made under the following assumptions: Reynolds number $N_{Re} = v_m r_0/\nu = 10^5$ and $\sigma = 1$, uniform profile of the axial velocity component, "solid body"-law profile of the tangential velocity component, linear profile of turbulence energy, uniform profile of turbulent viscosity ν_t, and $\nu_{ef} = 10^{-3}$. The results of these calculations are shown in Fig. 3. The graphs here indicate a generation of turbulence near the pipe wall. As the flow develops, the energy of this turbulence is transmitted from the pipe wall toward the center, which its profile with the peak shifting toward the pipe axis indicates. At the same time, energy is also dissipated and its profile acquires the characteristic features of a developed one. At higher values of the whirl parameter, turbulence energy is generated more intensively and the turbulent viscosity increases at the pipe wall so that the level of kinetic turbulence energy at the pipe entrance has a relatively lesser influence on the distributions of components of the average velocity in the stream. It ought to be noted, however, that stipulating k and ν_t profiles far from "natural" ones will drastically change the turbulence parameters within the initial pipe segment and thus can qualitatively distort the flow pattern.

NOTATION

z, r, θ, axial, radial, and tangential coordinates; r_0, pipe radius, v_z, v_r, v_θ, time-averaged components of velocity; v'_z, v'_r, v'_θ, corresponding fluctuation components of velocity; ν, coefficient of kinematic viscosity; $N_{Re} = v_m r_0/\nu$, Reynolds number; v_m, mean-discharge velocity; L, pipe length, α, angle between the velocity vector and direction θ; $\nu_{ef} = \nu + \nu_t$; V_*, dynamic velocity.

LITERATURE CITED

1. B. E. Launder and D. B. Spalding, Mathematical Models of Turbulence, No. 4, Academic Press, London (1972).
2. O. L. Anderson, "A comparison of theory and experiment for incompressible turbulent swirling flows in axisymmetric ducts," AIAA Paper No. 72-43 (1972).
3. G. E. Sturov, in: Some Problems in Study and Industrial Application of the Eddy Effect [in Russian], Kuibyshev. Aviats. Inst., Kuibyshev (1974), p. 211.
4. D. G. Lilley and N. A. Chigier, "Nonisotropic turbulent flows from mean-value distributions," Int. J. Heat Mass Transfer, 14, 573 (1971).
5. B. E. Launder and D. B. Spalding, "Numerical computation of turbulent flows," Computer Methods Appl. Mech. Eng., 3, No. 2 (1974).
6. A. D. Gosman, V. M. Pan, A. K. Ranchel, D. B. Spalding, and M. Wolfstein, Numerical Methods of Analyzing the Flow of Viscous Fluid [Russian translation], Mir, Moscow (1972).
7. R. G. Backshall and F. Landis, "The boundary-layer velocity distribution in turbulent swirling pipe flows," ASME Paper No. 69-FE-14 (1969).
8. J. Laufer, "The structure of turbulence in fully developed pipe flow," Report No. 1174, NASA (1954).

EFFECT OF MASS FORCES ON PARTICLE MOTION IN A LAMINAR SUBLAYER OF TURBULENT FLOW IN RECTILINEAR CHANNELS WITH VARIOUS SPATIAL ORIENTATIONS

Yu. M. Grishin and A. A. Mosin

UDC 532.517

Based on solutions of the equations of motion, features of motion of a liquid particle are analyzed for a laminar sublayer of turbulent flow in channels with varying spatial orientations.

It is well known [1] that in solving the problem of particle precipitation at channel walls in a turbulent gas flow, the transverse particle motion is advisably considered separately in the flow bulk and in a narrow boundary layer with a large velocity gradient – the laminar sublayer. In the bulk flow the particle motion is uniquely determined by the action of turbulent flow pulsations on the particles [2] and obeys the laws of turbulent diffusion. In the boundary-layer region the effect of diffusion particle motion is weakened in comparison with systematic effects (due to fundamental forces). In this case it was shown [3] that particle precipitation at the channel walls is primarily determined by particle trajectories in the laminar sublayer. Despite the large number of papers devoted to calculating particle trajectories in the laminar sublayer (see, e.g., [4]), the problem of the effect of mass forces (weight forces), taking into account their interactions with forces generated in the fluid itself, on trajectories of particle motion in channels with varying spatial orientations has so far not been sufficiently investigated.

In this connection we consider the problem of motion of nondeformed particles of spherical shape in a laminar sublayer of an evolving turbulent flow moving in a rectilinear channel. We assume that the basic parameters of the boundary layer are independent of the channel orientation in space, do not vary along the channel (stable flow), and are determined by the well-known semiempirical relations [5]

Translated from Inzhenerno-Fizicheskii Zhurnal, Vol. 37, No. 2, pp. 260-268, August, 1979. Original article submitted October 2, 1978.